JOURNAL OF GEOPHYSICAL RESEARCH, VOL. 115, A02215, doi:10.1029/2009JA014397, 2010

Phase relation between Pi2-associated ionospheric Doppler velocity and magnetic pulsations observed at a midlatitude MAGDAS station

Akihiro Ikeda,[1] Kiyohumi Yumoto,[2] Teiji Uozumi,[2] Manabu Shinohara,[3] Kenro Nozaki,[4] Akimasa Yoshikawa,[1] V. V. Bychkov,[5] and B. M. Shevtsov[5]

Received 27 April 2009; revised 28 December 2009; accepted 8 January 2010; published 27 February 2010.

[1] We examined the correlation between nighttime Pi2 pulsations detected simultaneously by a frequency modulated continuous wave (FM-CW) (HF) radar and by a ground magnetometer, both located at a midlatitude (L = 2.05) Magnetic Data Acquisition System station. Eighty-three Pi2 events were observed during the 43 day period from 23 September 2006 to 4 November 2006. The variations of the ground magnetic H component and ionospheric Doppler velocity (V^*) exhibited high coherence for 80% of the 83 Pi2 events, for about a half of which the H and V^* variations have the same dominant frequency. For such events, V^* led H by 90° in phase, in the midnight sector of 2230–0300 LT. The average Ey (east-west electric field) amplitude derived from V^* is 0.27 mV/m. The 90° phase delay was not found for the five events that were observed near dusk and dawn. The phase relation of H and V^* for Pi2s in the midnight sector may be explained in terms of the radial standing structure of compressional waves, i.e., cavity mode oscillation.

Citation: Ikeda, A., K. Yumoto, T. Uozumi, M. Shinohara, K. Nozaki, A. Yoshikawa, V. V. Bychkov, and B. M. Shevtsov (2010), Phase relation between Pi2-associated ionospheric Doppler velocity and magnetic pulsations observed at a midlatitude MAGDAS station, *J. Geophys. Res.*, *115*, A02215, doi:10.1029/2009JA014397.

1. Introduction

[2] At the onset of magnetospheric substorms, Pi2 magnetic pulsation is observed globally in the magnetosphere. Pi2 pulsation is an impulsive hydromagnetic oscillation and its period range is 40 to 150 s [e.g., *Saito and Matsushita*, 1968]. Pi2 pulsations have been attributed to different modes depending on the latitude and local time of observation [e.g., *Olson*, 1999; *Yumoto and the CPMN Group*, 2001]. In particular, low-latitude and midlatitude Pi2 pulsations, which are the subject of this paper, are explained in terms of the cavity mode resonance in the plasmasphere [e.g., *Sutcliffe and Yumoto*, 1991; *Yeoman and Orr*, 1989]. From a ground-satellite statistical study, *Takahashi et al.* [1995] found that magnetic Pi2 pulsations in the nightside sector at $L < 4$ are dominated by the poloidal components and suggested cavity mode as an explanation. Additionally, *Takahashi et al.* [2001] analyzed the magnetic field and electric field observed by the CRRES satellite. They indicated that the sources of Pi2 pulsations are poloidal standing waves inside the plasmasphere. Furthermore, their result on the spatial phase structure of electric and magnetic field supported cavity mode excited between two reflecting boundaries.

[3] It is known that ionospheric disturbances measured by high-frequency (HF) Doppler radar at low latitudes and midlatitudes often show a good correlation with the variations of geomagnetic field [e.g., *Chan et al.*, 1962]. To explain the pulsation associated with Doppler oscillations, *Poole et al.* [1988] suggested that the observed Doppler velocity can be expressed as

$$V^* = V_1 + V_2 + V_3 \tag{1}$$

This equation means that Doppler velocity oscillation V^* is driven by a combination of three mechanisms: (1) changes in the refractive index arising from its dependence on magnetic field intensity, requiring no bulk motion of electrons (magnetic mechanism: V_1), (2) vertical motion of the electron gas driven by the east-west electric field (advection mechanism: V_2), and (3) compression and rarefaction of the plasma by the field-aligned component of the wave magnetic field (compression mechanism: V_3). From midlatitude observations, *Grant and Cole* [1992] suggested that Pi2-associated Doppler velocity oscillation was caused by the

[1]Department of Earth and Planetary Sciences, Kyushu University, Fukuoka, Japan.
[2]Space Environment Research Center, Kyushu University, Fukuoka, Japan.
[3]Kagoshima National College of Technology, Kagoshima, Japan.
[4]National Institute of Information and Communications Technology, Koganei, Japan.
[5]Institute of Cosmophysical Research and Radiowaves Propagation, Far Eastern Branch, Russian Academy of Sciences, Kamchatka Region, Russia.

0148-0227/10/2009JA014397$09.00

V_2 mechanism. On the other hand, *Marshall and Menk* [1999] observed low-latitude nighttime Pi2-associated and irregular Pc4-associated Doppler velocity by HF radars. Their observation suggested that V_3 was dominant for the low-latitude nighttime Pi2 pulsations.

[4] Despite the previously demonstrated potential of HF radars in Pi2 research, Doppler radar study of Pi2 pulsations is limited. We believe that more extensive use of the radar will lead to a better understanding of Pi2 pulsations in the ionosphere. In the present paper, we examined the phase relation between the ionospheric Doppler velocity in the ionospheric *F* region detected by a frequency modulated continuous wave (FM-CW) radar and magnetic Pi2 pulsations observed by the Magnetic Data Acquisition System (MAGDAS). In addition, we estimated the ionospheric electric field intensity from the observed Doppler velocity.

[5] This paper is organized as follows: introduction of the data and observational instruments is in section 2, descriptions of the observational results are in section 3, and discussion and conclusion are in section 4.

2. Observation

2.1. FM-CW Radar Data

[6] The present study is based on the data from an FM-CW radar located at Paratunka, Kamchatka region, Russia (PTK: magnetic latitude, 45.8°; magnetic longitude, 221.6°; L = 2.05; LT = UT + 10.5 h). The FM-CW radar is a type of HF radar that can measure the range of target as well as Doppler shift of the target by using the following method. We target the ionospheric *F* region for Doppler measurement. Our radar is an improved version of the FM-CW radar developed by *Nozaki and Kikuchi* [1987, 1988].

[7] Generally, FM-CW radars sweep their transmitting frequency. In the case of our Doppler observation for this study, the range of frequency sweep was from 3.00 MHz to 3.01 MHz. By using an FM-CW radar, *Poole* [1985] and *Poole and Evans* [1985] made the Doppler observation for the first time. They used three-cell sounding. By contrast, our Doppler observation is based on a fast Fourier transform (FFT) technique, which is a variation of the technique developed by *Barrick* [1973] to measure ocean waves. In this technique, the range and Doppler shift can be estimated using a double FFT algorithm. The first FFT over each frequency sweep yields the range information, and the second FFT for each range bin over a number of frequency sweeps provides the Doppler frequency. In contrast to the three-cell sounding, which requires the sweep frequency to be changed three times in each duty cycle, the FFT method has the advantage that the sweep range of frequency is steady and remains constant.

[8] With our radar system, we are able to measure the vertical drift velocity of the ionized layer and its virtual height [*Ikeda et al.*, 2008]. The velocity of the transmitted signal is lower than *c* (velocity of light) because the path of the signal is not in a vacuum and the calculated height of the reflection point is higher than the actual height. Therefore the height information provided by our FM-CW radar is virtual height. The observed Doppler frequency Δf is given by

$$\Delta f = f_0 \times 2V^* / c \tag{2}$$

where V^* is the drift velocity vertical to the surface of the earth and f_0 is the transmitting frequency. Thus V^* of the ionosphere is given by

$$V^* = c \times \Delta f / 2 f_0 \tag{3}$$

[9] We use 3.0 MHz for the transmitting frequency f_0 at night. The data is digitized with 3 s sampling, and the accuracy of the vertical drift velocity is 3.9 m/s at 3.0 MHz.

2.2. Geomagnetic Field Data

[10] One second magnetic data from the fluxgate magnetometer at PTK was used for comparison with the radar data. The distance between the magnetometer and the radar is about 500 m. This station is a part of the Magnetic Data Acquisition System of the Circumpan Pacific Magnetometer Network (MAGDAS/CPMN) [*Yumoto and the MAGDAS Group*, 2006, 2007]. The details of this network are available at the Space Environment Research Center (SERC) Web page (http://www.serc.kyushu-u.ac.jp/index_e.html).

[11] To detect substorms, we used data from high-latitude MAGDAS/CPMN magnetometers at Macquarie Island, Australia (MCQ: magnetic latitude, −65.54°; magnetic longitude, 248.12°; L = 5.41; LT = UT + 10.6 h) and at Kotel'nyy, Russia (KTN: magnetic latitude, 69.92°; magnetic longitude, 201.03°; L = 8.62; LT = UT + 9.2 h). The AL index, which was provided by the World Data Center for Geomagnetism, Kyoto, was also used.

[12] To be consistent with previous studies that defined Pi2 as a phenomenon associated with substorms, we targeted Pi2 events which were associated with substorms. In this paper, we chose Pi2 events that show a sudden decrease in the AL index ($\Delta AL \leq -50$ nT) and the negative bay ($\Delta H \leq -50$ nT) in *H* at high-latitude stations MCQ or KTN. We chose also events showing either $\Delta AL \leq -50$ nT or $\Delta H \leq -50$ nT.

3. Analysis

3.1. Case Studies

[13] Figure 1 shows an example of a nighttime Pi2 event that was observed on 29 October 2006 when PTK was located in the premidnight sector (2304–2316 LT). The first panel shows the ground magnetic horizontal northward component (*H*) and the second panel shows downward Doppler velocity (V^*) obtained by the FM-CW radar. The V^* defined positive downward through this paper. During this event, V^* was observed at the virtual height of about 300 km. The third and fourth panels show the corresponding band-pass-filtered (40–150 s) *H* and V^*, respectively. Pi2 pulsations were observed simultaneously in *H* and V^* in association with a positive bay in *H* that occurred around 1239 UT. The band-pass-filtered data show that the *H* oscillated with a peak-to-peak amplitude of 3.6 nT, and V^* with a peak-to-peak amplitude of 15.1 m/s. The vertical dashed lines indicate the peak times of the band-pass-filtered *H*. Using the vertical dashed lines that mark the timing of the peaks of the band-pass-filtered *H*, we find that the phase of *H* is shifted from V^*.

[14] To quantify the relationship between *H* and V^* pulsations, we used power spectral analyses. In the spectral analysis we obtained the power spectral density (PSD) using FFT. We applied FFT to the band-pass-filtered data. We used

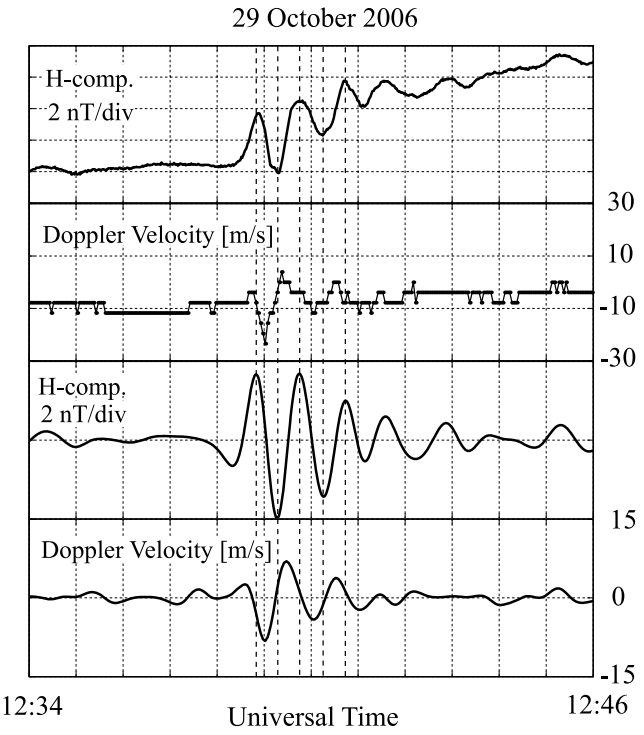

Figure 1. Example of a Type A Pi2 event observed by the MAGDAS magnetometer and the FM-CW radar on 29 October 2006 at PTK. Shown are H, V^*, the band-pass-filtered (40–150 s) data of H, and the band-pass-filtered (40–150 s) data of V^*.

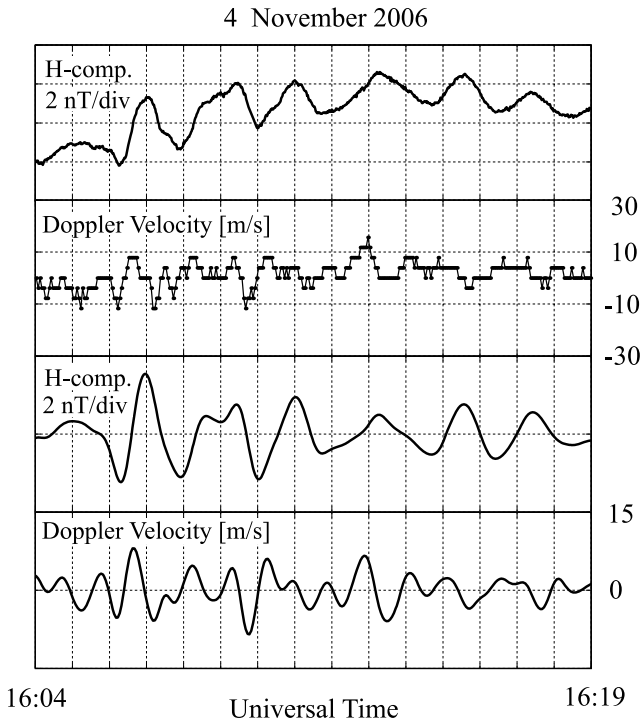

Figure 2. Same as Figure 1 for a Type B Pi2 event on 4 November 2006.

512-point FFT with a resolution of 1.3 mHz. A dominant spectral peak occurred at 16.9 mHz in both H (denoted F_H) and V^* (denoted F_V). In addition we calculated coherence and phase difference between H and V^*. We found that coherence at F_H (denoted $C(F_H)$) is 0.99 and V^* lead H by 91° at F_H. We will denote events having such features ($C(F_H) \geq 0.6$ and $F_H = F_V$) as Type A events.

[15] Next we consider another Pi2 event that occurred on 4 November 2006. The wave forms in Figure 2 are again H, V^*, filtered H, and filtered V^*. The virtual height of this observation was about 250 km. In this event, the dominant frequency of H is 7.8 mHz, but the dominant frequency of V^* is 19.5 mHz. The $C(F_H)$ is 0.98. This event can be classified as high coherence ($C(F_H) \geq 0.6$) but the dominant frequency is a mismatch ($F_H \neq F_V$). Hereafter, we denote such events as Type B events.

[16] The final Pi2 event, shown in Figure 3, occurred on 19 October 2006. In this event, the FM-CW radar observed the region at 250 km (virtual height). The $C(F_H)$ is 0.52 for this event. Hereafter, we denote such low-coherence ($C(F_H) < 0.6$) events as Type C events.

3.2. Event Selection and Occurrence

[17] To determine whether the phase shift between H and V^* occur around a particular value, we examined Pi2 events statistically. Pi2 events were selected from the band-pass-filtered (40–150 s) H for PTK during the interval from 23 September 2006 to 4 November 2006. We first selected Pi2 events exhibiting amplitude larger than 1 nT that occurred

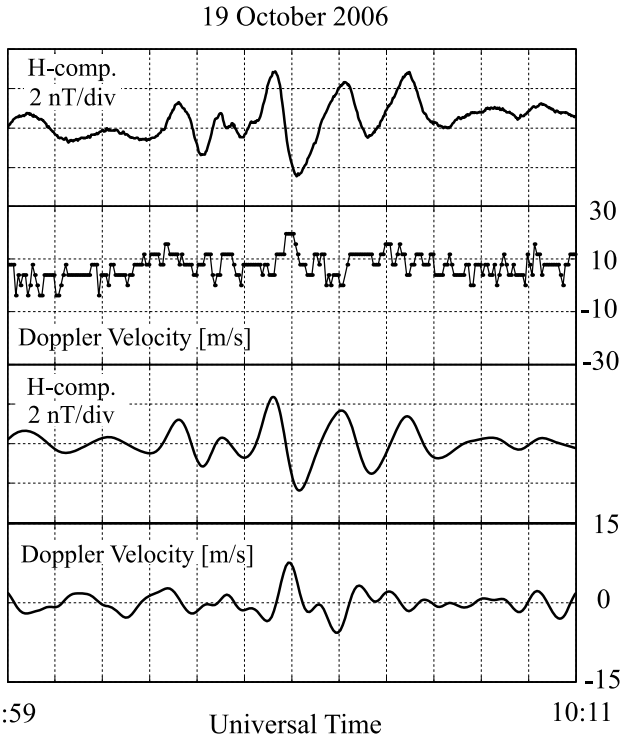

Figure 3. Same as Figure 1 for a Type C Pi2 event on 19 October 2006.

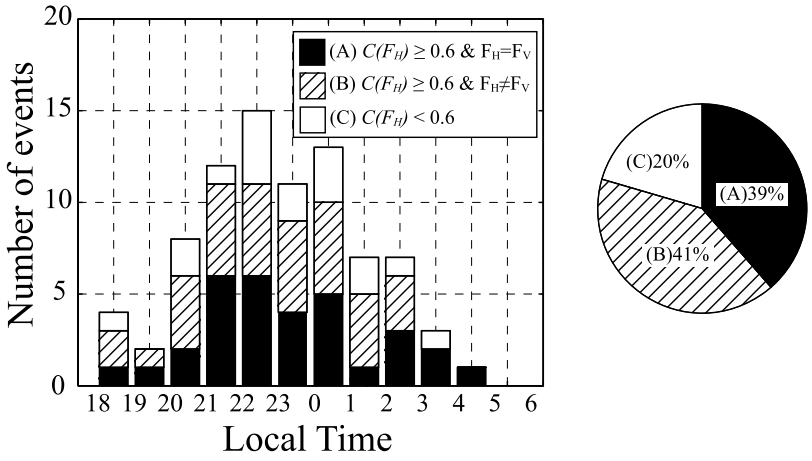

Figure 4. Occurrence of the Pi2 events detected by the MAGDAS magnetometer and the FM-CW radar and relative percentage of Type A events (black; $C(F_H) \geq 0.6$ and $F_H = F_V$), Type B events (hatched; $C(F_H) \geq 0.6$ and $F_H \neq F_V$), and Type C events (white; $C(F_H) < 0.6$).

when the FM-CW radar was located on the nightside (1800–0600 LT) and observed the ionized layer at a height greater than 200 km. In addition, we checked if Pi2 events were associated with substorms. Identification of substorms is explained in section 2.2. Thus we found 83 Pi2 events. Their local time distribution is shown in Figure 4. The Pi2 events frequently occurred at midnight, rarely occurred on the duskside and the dawnside.

[18] Second, we took time segments of the Pi2 events which range from 10 to 20 minutes and calculated the PSD of H and V^* and examined the peak frequency of H, denoted F_H, and the peak frequency of V^*, denoted F_V, respectively. If there are more than one peaks, we took a peak of the highest power. Also we calculated the coherence between H and V^* to determine the coherence at F_H (denoted $C(F_H)$). Last, we classified all events into 3 types: Type A, $C(F_H) \geq 0.6$ and $F_H = F_V$; Type B, $C(F_H) \geq 0.6$ and $F_H \neq F_V$; and Type C, $C(F_H) < 0.6$. Consequently, we found 32 Type A events, 34 Type B events and 17 Type C events. The local time distribution and occurrence frequency of the 3 types are shown in Figure 4. In Figure 4, Type A, B and C are shown by black bars, hatched bars and white bars, respectively. We can see that H and V^* variations showed high coherence ($C(F_H) \geq 0.6$) for 80% of the 83 Pi2 events, for about a half of which the H and V^* variations have the same dominant frequency ($F_H = F_V$).

3.3. Phase Relation

[19] In this study, we focus on the Type A events ($C(F_H) \geq 0.6$ and $F_H = F_V$). Figure 5 shows the phase delay between H and V^* for the 32 Type A Pi2 events. The phase delay was obtained at the most dominant frequency of each event. Here, the negative phase means V^* leads and positive phase means H leads. It should be noted that the Pi2 phase delay is mostly near −90° in the midnight sector of 2230–0300 LT. The average phase delay during the midnight sector is −84.68° and its standard deviation is 25.2. Before that, the phase delay changed from near 90° to near −90° around 2100–2200 LT. In the dusk sector (1800–2100 LT) and dawn sector (0300–0600 LT), 5 out of 8 events were between 30° and 150°, which clearly separated from the events observed near midnight.

4. Discussion and Conclusion

[20] We have examined the correlation between the nighttime Pi2 pulsations detected simultaneously by an FM-CW (HF) radar and by the MAGDAS magnetometer at PTK (L = 2.05). Our results are summarized as follows. (1) A total of 83 Pi2 events were found during a 43 day period from 23 September 2006 to 4 November 2006. 66 out of these showed high coherence ($C(F_H) \geq 0.6$) between H and V^*. (2) 32 out of the high-coherence events have the same dominant frequency in H and V^* ($F_H = F_V$). (3) For these events, which are called Type A events in the present paper,

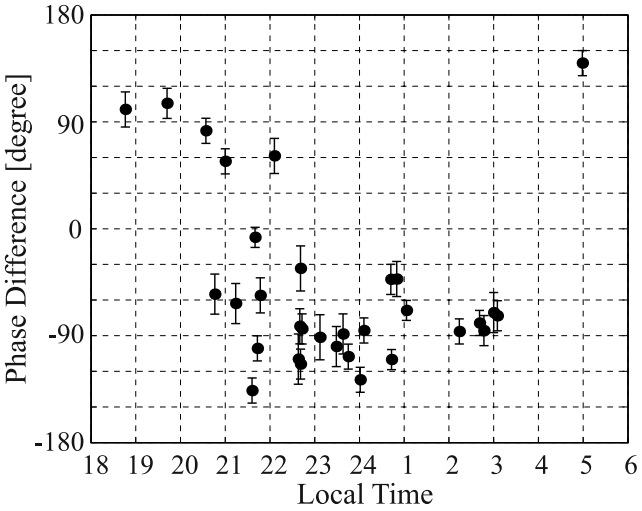

Figure 5. Local time distribution of the Pi2 phase difference between H and V^* at PTK for the Type A events. The phase delay was obtained at the most dominant frequency of each event. The error bars indicate the uncertainty of the phase difference caused by the time resolution of the data (3 s).

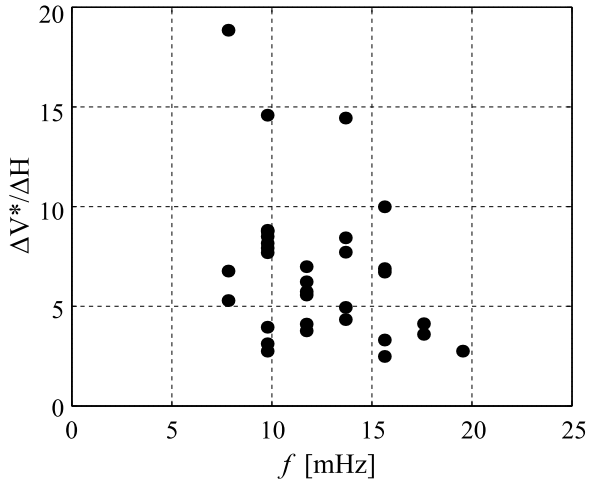

Figure 6. Scatterplot of the normalized amplitude of the Doppler velocity ($\Delta V^*/\Delta H$) with its pulsation frequency (f) for the Type A Pi2 events.

V^* led H in phase by ~90° if observed in the midnight sector (2230–0300 LT). (4) In the dusk sector (1800–2100 LT) and the dawn sector (0300–0600 LT), 5 out of 8 events did not show phase difference of −90° between H and V^*. Previous studies [e.g., *Marshall and Menk*, 1999] did not reveal the existence of these features.

[21] As indicated in equation (1), oscillations in Doppler velocity V^* arise from three possible mechanisms: (1) magnetic mechanism V_1, (2) advection mechanism V_2, and (3) compression mechanism V_3 [*Poole et al.*, 1988; *Sutcliffe and Poole*, 1989]. *Sutcliffe and Poole* [1990] theoretically evaluated the amplitude of V^*, V_1, V_2 and V_3 for oscillations in the Pc3 band. They assumed that the Pc3 waves are purely Alfvénic. In their analysis, the main cause of V^* pulsations at nighttime was found to be the V_2 and V_3 mechanisms, because low Pedersen and Hall conductivities at nighttime enhance the pulsation electric field. Using vertical HF soundings of bottomside F layer disturbances associated with midlatitude Pi2 pulsations, *Grant and Cole* [1992] showed that the amplitude of the observed Doppler velocity oscillation was constant with height and argued that the V_2 mechanism was dominant. Here, V_2 is due to the vertical motion driven by an east-west pulsation electric field. On the other hand, *Marshall and Menk* [1999] reported that the low-latitude nighttime Pi2-associated and irregular Pc4-associated ΔF (amplitude of the Doppler frequency) was proportional to the pulsation frequency (f). Specifically they showed that the $\Delta F/\Delta H$ ratio was proportional to f, where ΔH is the pulsation amplitude of H. This relation indicates that V_3 was dominant for the low-latitude nighttime Pi2, because V_3 is directly proportional to the pulsation frequency f, while V_2 is not (details were shown by *Poole et al.* [1988]).

[22] In order to determine which of V_2 and V_3 mechanisms is dominant for Pi2 events, we compared ΔV^* and f obtained by our FM-CW radar. We note that ΔV^* is an amplitude of V^* pulsation and is directly proportional to ΔF as indicated by equation (2). Figure 6 shows the dependence of the $\Delta V^*/\Delta H$ ratio on f for the Type A Pi2 events. We can clearly see that the $\Delta V^*/\Delta H$ ratio does not depend on f. This result suggests that the Doppler velocity for the Type A Pi2 events is due to the east-west pulsation electric field (V_2) in the nightside. The result of *Marshall and Menk* [1999] might be associated with Type B and C events described in the present paper.

[23] From the above discussion, we can estimate the intensity of the pulsation electric field in the ionosphere. The Pi2 event on 29 October 2006 (Figure 1) had a ΔV^* peak-to-peak amplitude of 15.1 m/s. For the rough estimate of the electric field intensity, we calculated the east-west electric field intensity Ey by using the frozen-in equation

$$\mathbf{E} = -\mathbf{V} \times \mathbf{B} \tag{4}$$

We get $\mathbf{E}$ (directed in the y direction) by substituting $\mathbf{V} = \mathbf{\Delta V^* e_z}$ and $\mathbf{B} = \mathbf{H e_H}$ to equation (4), where $\mathbf{e_z}$ is the unit vector pointing vertically upward and $\mathbf{e_H}$ is the unit vector in the direction of the magnetic field projected on the Earth Surface. For the event on 29 October 2006, we get 0.29 mV/m in the ionospheric F region. The average amplitude of Ey for the 32 Type A events that were associated with substorms is 0.27 mV/m. If we look at only the 19 out of 32 events that occurred in the midnight sector (2230–0300 LT), we also obtain the average amplitude of 0.27 mV/m.

[24] The plasmaspheric cavity mode has been proposed as a model for low-latitude Pi2 pulsations. We examine whether our observations can be explained by the model. *Takahashi et al.* [2001] illustrated the radial mode structure of a cavity mode excited in a simple box model which shows the amplitude and phase of Ey (electric field azimuthal component) and Bz (magnetic field compressional component) between the inner boundary and the outer boundary. The fundamental mode of Bz and Ey has half a wave length between the two boundaries. The node (antinode) of Bz (Ey) is located at the center of the two boundaries. At both boundaries, there is an antinode (node) of Bz (Ey). The cross phase between Bz and Ey is either +90° or −90° depending on the position relative to the boundaries. Inside the plasmasphere ($L < 4$), magnetic and electric field data obtained by the CRRES satellite showed consistency with the simple box model [*Takahashi et al.*, 2001]. Also, *Han et al.* [2004] reported that magnetic Pi2 pulsations observed simultaneously above (the Ørsted satellite) and below (ground) the ionosphere were consistent with the cavity mode model. They found that nighttime Pi2 waves observed by the low-altitude satellite (h = 638 ~ 849 km) Ørsted and at KAK (L = 1.26) oscillated without phase lag at nighttime.

[25] According to the box model of *Takahashi et al.* [2001], Ey leads Bz by 90° near the inner boundary. This is consistent with our result of the phase delay between H and V^* for the Type A Pi2 events observed in the local time sector of 2230–0300 LT (see Figure 5). Therefore we suggest that the Type A Pi2 events are compressional standing waves, i.e., the cavity mode, and that the electric field oscillation in the ionospheric F region is a manifestation of the cavity mode resonance at midnight.

[26] The Ey amplitude derived from our observation also fits the cavity mode model. *Takahashi et al.* [1999] reported the electric field amplitude measured by the CRRES satellite for plasmaspheric Pi2 pulsations. Their Pi2 event had a peak-to-peak amplitude of more than 1 mV/m in the dawn-dusk component at L = 4.8 and MLT = 21.8 [see *Takahashi et al.*,

1999, Figure 5]. For our Type A Pi2 events observed in the 2230–0300 LT sector, the average peak-to-peak *Ey* amplitude in the ionospheric *F* region is 0.27 mV/m, which is much smaller than the electric field amplitude observed by the CRRES satellite inside the plasmasphere. This is consistent with the simple cavity mode model by *Takahashi et al.* [2001], since in that model *Ey* has a node at the ionosphere and an antinode of *Ey* is located close to the plasmapause [*Takahashi et al.*, 2003].

[27] There are satellite observations away from midnight that support the cavity mode model. *Nosé et al.* [2003] studied a morningside Pi2 event and concluded that the pulsation was caused by the plasmaspheric cavity mode resonance. *Han et al.* [2004] showed that the Pi2 pulsations at both the dawnside and duskside were due to the cavity mode. In the present study, we have three event in the dawn sector (0300–0600 LT), and we have five events in the dusk sector (1800–2100 LT). Among these events three out of eight events showed a ~90° phase delay of *H* from *V** consistent with the cavity mode, but other five events did not indicate the phase delay of a radial standing wave. It seems that the radial structure of a cavity mode is confined to the midnight sector.

[28] We should also comment on previous studies relevant to our Type B events ($C(F_H) \geq 0.6$ and $F_H \neq F_V$) and Type C events ($C(F_H) < 0.6$). *Marshall and Menk* [1999] detected high-coherence Pc3-4 events when the radio transmitting frequency f_0 was close to f_oF_2. This fact may be related to the occurrence of Type C events. For the event which showed mismatch of the dominant frequency between *H* and *V** ($F_H \neq F_V$), the Doppler oscillation is possibly driven not only by local perturbations but also by disturbances of polar origin. Magnetic field oscillations of the polar origin effects have been observed by in a low-latitude ionospheric Doppler observation in the Pc5 band [*Motoba et al.*, 2004]. In the future, we need to study these events by including high-latitude magnetic field data.

[29] In conclusion, our FM-CW radar and MAGDAS observations show that the Doppler velocity for Type A events at midlatitude (L = 2.05) is likely caused by the east-west pulsation electric field (*Ey*). The phase relation between *H* and *V** near midnight is consistent with a simple cavity mode model [*Takahashi et al.*, 2001] and implies that the midlatitude Type A Pi2 pulsation is a radially standing wave. Furthermore, the average *Ey* amplitude (0.27 mV/m) for Type A Pi2 events near midnight is consistent with the cavity-mode Pi2s compared with the electric field observation by CRRES inside the plasmasphere [*Takahashi et al.*, 1999].

[30] In order to further understand midlatitude Pi2 pulsations, it is necessary to examine the correlation between the magnetic *D* component and *V**. This is because *Lester et al.* [1983] showed that Pi2 pulsations at midlatitudes (M.Lat = 55°) appear in both *H* and *D* components. They explained the midlatitude Pi2 pulsations by an oscillation of the substorm current wedge (SCW) instead of a cavity mode.

[31] **Acknowledgments.** The work for this paper was supported by JSPS as the Grant-in-Aid for Overseas Scientific Survey (18253005) and in part by National Institute of Information and Communications Technology (NICT). We also acknowledge World Data Center for Geomagnetism, Kyoto (http://swdcwww.kugi.kyoto-u.ac.jp/index.html), for calculating IGRF model and providing auroral electrojet indices.

[32] Zuyin Pu thanks the reviewers for their assistance in evaluating this paper.

References

Barrick, D. E. (1973), FM/CW radar signals and digital processing, *NOAA Technical Rep. ERL 283-WPL 26*, NOAA, Boulder, Colo.

Chan, K. L., D. P. Kanellakos, and O. G. Villard Jr. (1962), Correlation of short-period fluctuations of the Earth's magnetic field and instantaneous frequency measurements, *J. Geophys. Res.*, *67*, 2066–2072.

Grant, J. F., and K. D. Cole (1992), The height dependence of the perturbation of the mid-latitude F-region by Pi2 pulsations, *Planet. Space Sci.*, *40*, 1461–1477.

Han, D.-S., T. Iyemori, M. Nosé, H. McCreadie, Y. Gao, F. Yang, S. Yamashita, and P. Stauning (2004), A comparative analysis of low-latitude Pi2 pulsations observed by Ørsted and ground stations, *J. Geophys. Res.*, *109*, A10209, doi:10.1029/2004JA010576.

Ikeda, A., K. Yumoto, M. Shinohara, K. Nozaki, A. Yoshikawa, and A. Shinbori (2008), SC-associated ionospheric electric fields at low latitude: FM-CW radar observation, *Mem. Fac. Sci. Kyushu Univ., Ser. D*, *XXXII*(1), 1–6.

Lester, M., W. J. Hughes, and H. Singerm (1983), Polarization patterns of Pi2 magnetic pulsations and the substorm current wedge, *J. Geophys. Res.*, *88*, 7958–7966.

Marshall, R. A., and F. W. Menk (1999), Low latitude observations of Pc3-4 and Pi2 geomagnetic pulsations in the ionosphere, *Ann. Geophys.*, *17*, 1397–1410.

Motoba, T., T. Kikuchi, T. F. Shibata, and K. Yumoto (2004), HF Doppler oscillations in the low-latitude ionosphere coherent with equatorial long-period geomagnetic field oscillations, *J. Geophys. Res.*, *109*, A06214, doi:10.1029/2004JA010442.

Nozaki, K., and T. Kikuchi (1987), A new multimode FM/CW ionosonde, *Mem. Natl Inst. Polar Res., Spec. Issue*, *47*, 217–224.

Nozaki, K., and T. Kikuchi (1988), Preliminary results of the multimode FM/CW ionosonde experiment, *Proc. NIPR Symp. Upper Atmos. Phys.*, *1*, 204–209.

Nosé, M., et al. (2003), Multipoint observations of a Pi2 pulsation on morningside: The 20 September 1995 event, *J. Geophys. Res.*, *108* (A5), 1219, doi:10.1029/2002JA009747.

Olson, J. V. (1999), Pi2 pulsations and substorm onsets: A review, *J. Geophys. Res.*, *104*, 17,499–17,520.

Poole, A. W. V. (1985), Advanced sounding: 1. The FMCW alternative, *Radio Sci.*, *20*, 1609–1616.

Poole, A. W. V., and G. P. Evans (1985), Advanced sounding: 2. First results from an advanced chirp ionosonde, *Radio Sci.*, *20*, 1617–1623.

Poole, A. W. V., P. R. Sutcliffe, and A. D. M. Walker (1988), The relationship between ULF geomagnetic pulsations and ionospheric Doppler observations: Derivation of a model, *J. Geophys. Res.*, *93*, 14,656–14,664.

Saito, T., and S. Matsushita (1968), Solar cycle effects on geomagnetic Pi2 pulsations, *J. Geophys. Res.*, *73*, 267–286.

Sutcliffe, P. R., and A. W. V. Poole (1989), Ionospheric Doppler and electron velocities in the presence of ULF waves, *J. Geophys. Res.*, *94*, 13,505–13,514.

Sutcliffe, P. R., and A. W. V. Poole (1990), The relationship between ULF geomagnetic pulsations and ionospheric Doppler oscillations: Model predictions, *Planet. Space. Sci.*, *38*, 1581–1589.

Sutcliffe, P. R., and K. Yumoto (1991), On the cavity mode nature of low-latitude Pi2 pulsations, *J. Geophys. Res.*, *96*, 1543–1551.

Takahashi, K., S.-I. Ohtani, and B. J. Anderson (1995), Statistical analysis of Pi2 pulsation observed by the AMPTE CCE spacecraft in the inner magnetosphere, *J. Geophys. Res.*, *100*, 21,929–21,941.

Takahashi, K., S. Ohtani, W. J. Hughes, R. R. Anderson, and S. I. Solovyev (1999), CRRES satellite observations associated with low-latitude Pi2 pulsations, *J. Geophys. Res.*, *104*, 17,431–17,440.

Takahashi, K., S. Ohtani, W. J. Hughes, and R. R. Anderson (2001), CRRES satellite observations associated with low-latitude Pi2 pulsations, *J. Geophys. Res.*, *106*, 15,567–15,581.

Takahashi, K., D.-H. Lee, M. Nosé, R. R. Anderson, and W. J. Hughes (2003), CRRES electric field study of the radial mode structure of Pi2 pulsations, *J. Geophys. Res.*, *108*(A5), 1210, doi:10.1029/2002JA009761.

Yeoman, T. K., and D. Orr (1989), Phase and spectral power of mid-latitude Pi2 pulsations: Evidence for a plasmaspheric cavity resonance, *Planet. Space Sci.*, *38*, 1367–1383.

Yumoto, K., and the CPMN Group (2001), Characteristics of Pi 2 magnetic pulsations observed at the CPMN stations: A review of the STEP results, *Earth Planets Space*, *53*, 981–992.

Yumoto, K., and the MAGDAS Group (2006), MAGDAS project and its application for space weather, in *The Solar Influence on the Heliosphere*

and Earth's Environment: Recent Progress and Prospects, edited by N. Gopalswamy and A. Bhattacharyya, Quest, Mumbai, India.

Yumoto, K., and the MAGDAS Group (2007), Space weather activities at SERC for IHY: MAGDAS, *Bull. Astron. Soc. India*, *35*, 511–522.

V. V. Bychkov and B. M. Shevtsov, Institute of Cosmophysical Research and Radiowaves Propagation, Far Eastern Branch, Russian Academy of Sciences, 7. Mirnaya str. Paratunka, Elizovskiy District, Kamchatka Region 684034, Russia.

A. Ikeda and A. Yoshikawa, Department of Earth and Planetary Sciences, Kyushu University, 6-10-1 Hakozaki, Fukuoka 812-8581, Japan. (a-ikeda@geo.kyushu-u.ac.jp)

K. Nozaki, National Institute of Information and Communications Technology, 4-2-1 Nukui-Kitamachi, Koganei, Tokyo 184-8795, Japan.

M. Shinohara, Kagoshima National College of Technology, 1460-1 Shinkou Hayato-cho, Kagoshima 899-5193, Japan.

T. Uozumi and K. Yumoto, Space Environment Research Center, Kyushu University, 6-10-1 Hakozaki, Fukuoka 812-8581, Japan.